Application of Time-Resolved Linear Dichroism Spectroscopy: Relaxation of Excited Hexamethylbenzene/1,2,4,5-Tetracyanobenzene Charge-Transfer Complexes

Bradley R. Arnold,* Alexander W. Schill, and Pavel V. Poliakov

Department of Chemistry and Biochemistry, University of Maryland, Baltimore County, Baltimore, Maryland 21250

Received: August 1, 2000; In Final Form: October 24, 2000

The charge-transfer complex formed between hexamethylbenzene and 1,2,4,5-tetracyanobenzene has been studied using time-resolved linear dichroism spectroscopy. These studies allowed the angle between the transition moment vectors for the absorptions of the ground-state charge-transfer complex and the product contact-radical ion pair to be measured. The results were compared with predictions based on the Mulliken two-state model and an assumed structure of the ground-state complex. The comparison between the observed and predicted angles supports the notion that relaxation of the excited charge-transfer complex leads to a change in the complex geometry. The time dependence of the dichroism allows the average rotational diffusion time constant to be determined. For this complex in 1,2-dichloroethane at room temperature, $\tau_{OR} = 75$ ps. This value is comparable to what would be expected based on Debye−Stokes−Einstein diffusion theory at the stick boundary limit.

Introduction

Current interest in the photochemistry and photophysics of charge-transfer (CT) complexes stems from the fact that rapid electron-transfer reactions, and processes initiated by these reactions, may be studied in the absence of relatively slow diffusional quenching processes.[1] The formation of these complexes plays a significant role in many organic and inorganic reaction mechanisms as well as numerous important biological processes.[2−4] Because of the widespread applications of CT complexes, an understanding of the initial excitation and electron-transfer processes could have ramifications in areas ranging from the design of photoelectric devices to photography and lithography.[2−4]

Popular belief suggests that absorption of a photon in the CT band of the complex leads directly to ion-pair formation in accordance with the Mulliken two-state model.[3,5−7] This belief has been brought into question in a series of papers where a rapid relaxation of an initially formed intermediate has been observed.[8−13] The formation of loose ion pairs,[14] multiple ground and excited states,[15,16] and 2:1 exciplexes and other relaxation processes have also been reported.[17−28] These findings indicate that the current belief may be severely oversimplified.

The rapid relaxation of the initially formed intermediate has been described as a delay in the formation of the charge-separated state[8−10] and as a relaxation from a Franck−Condon to a "relaxed" contact-radical ion pair (CRIP).[13] The difference between these two descriptions is more than semantic. In the first description, the relaxation and electron-transfer processes occur simultaneously, whereas in the second, the electron-transfer precedes relaxation. These interpretations, and thus the ramifications of either interpretation, have yet to be tested fully. In the following report, we will refer to the initial excited state as the Franck−Condon (FC) intermediate and assume the relaxed state is a CRIP.

* To whom correspondence should be addressed. Phone: (410) 455-2503. E-mail: barnold@umbc.edu.

What has been lacking in the descriptions of these relaxation processes is a detailed understanding of the electronic states involved in the ground- and excited-state reactivity of these complexes. Direct evaluation of CT absorption spectra does not allow a complete description of these states to be unambiguously established. These spectra are usually broad and featureless with significant band overlap. Observations of small differences between spectra are usually open to alternative interpretations, and a unique explanation is difficult to justify.

On the other hand, transition moment vector (TMV) directions are very sensitive to changes in the electronic configurations and ground-state structure even when the transition energies are not.[29,30] If the TMV directions could be measured, they may reveal details about the absorbing species that are otherwise hidden in the absorption spectrum.

The measurement of TMV directions is generally accomplished using linear dichroism spectroscopy on (partially) oriented samples, and there are numerous examples of measurements on single crystals or molecules dissolved in liquid-crystalline solvents, stretched-polymer samples, membranes and bilayers, or samples under the influence of electric fields.[29,30] The introduction of ultrafast lasers to spectroscopy has allowed polarization-specific spectroscopic information to be obtained in solution using time-resolved linear dichroism (TRLD) spectroscopy. The anisotropic nature of light absorption is used to produce partially oriented samples of excited states by a process known as photoselection.[29−33] When isotropic solutions are irradiated with light linearly polarized along the laboratory Z axis, uniaxially oriented samples of excited states are produced. If such samples are subsequently probed with a second beam of linearly polarized light of wavelength λ, before the samples have time to reorient, the measured absorbances obtained when the electric vector of the probe beam is parallel ($OD_{Z(\lambda)}$) compared to when it is perpendicular ($OD_{Y(\lambda)}$) to the laboratory Z axis may be different. The ratio of the polarized absorbances at wavelength λ, at any time, is defined as the dichroic ratio $d_\lambda = OD_{Z(\lambda)}/OD_{Y(\lambda)}$. It is convenient to describe

10.1021/jp002753d CCC: $20.00
Published on Web 12/20/2000

uniaxial orientation in terms of orientation factors as opposed to other, perhaps better known, order parameters.[29,30] Under the assumption that the sample is made up of linear absorbers with no overlapping transitions, the orientation factor for the *i*th transition is obtained from the dichroic ratio using the expression $K_i = d_\lambda/(d_\lambda + 2)$. The magnitude of K_i reflects both the extent of alignment of the sample and the angle between the initial absorption TMV and the probe TMV within the molecular frame. The degree of alignment of the sample is also reflected in the magnitude of the principal orientation factors, K_X, K_Y, and K_Z. Under the assumption that the bleaching of the ground state is negligible, the principal orientation factors for linear absorbers are given by photoselection theory: $K_Z = 0.60$ and $K_X = K_Y = 0.20$.[29,30] Once the principal orientation factors are established, eq 1 allows the absolute value of the angle between the excitation TMV and the probe TMV to be calculated.

$$|\theta| = \tan^{-1}\sqrt{\frac{K_Z - K_i}{K_i - K_Y}} \qquad (1)$$

The information gleaned from these experiments can be used to study molecular structure or solution dynamics and in the study of the topochemistry of molecular reactions.[33] As is used in the present context, topochemistry is concerned with the molecular movements required to convert reactants into products and how this movement changes the position of the product in space. As the reactant moves along a reaction coordinate, internal and external (i.e., solvent) interactions dictate not only the connectivity of the product but also its final orientation. TRLD provides a partial description of the topochemistry which can be used to place restrictions on possible reaction mechanisms.[20,34−37]

What is described below is an application of TRLD spectroscopy to the study of the hexamethybenzene (HMB)/1,2,4,5-tetracyanobenzene (TCNB) CT complex in solution. The angle between the TMV directions for the ground- and excited-state absorptions was determined experimentally and compared with the angle expected on the basis of Mulliken two-state theory. The relative orientation of the ground-state complex to the CRIP was resolved, and the topochemistry of the excited-state relaxation was examined.

Experimental Section

Methods. The picosecond pump−probe apparatus used in these experiments has been described in detail elsewhere[38] and will be described here only briefly. A Continuum PY61C Nd:YAG laser was used to produce 1064 nm pulses of ca. 35 ps in duration. The fundamental was doubled and subsequently tripled to produce 355 nm pulses to be used to excite the sample. Alternatively, excitation using 394 or 443 nm light was also possible by scattering the 355 nm light through a 25 cm solution cell of cyclohexane and isolating the stimulated Raman emission. Continuum was produced by focusing the residual 1064 nm light into a 10 cm quartz cell containing a 1:1 mixture of D_2O/H_2O. The resultant continuum pulse was spatially filtered, collimated, passed through a polarizer, and split into two beams, one of which was used as a reference beam while the other passed through the sample. Both reference and sample beams were coupled into separate legs of a bifurcated fiber-optic bundle and dispersed using a spectrograph/monochromator. A dual diode array was used to obtain transient spectra, and matched PMT detectors were used for single-wavelength kinetic measurements. The typical instrument response time was 30−45 ps, assuming Gaussian profiles. An IBM-compatible computer allowed automated control of the experiment through serial and general-purpose interface bus (GPIB) interfaces in addition to data storage and manipulation.

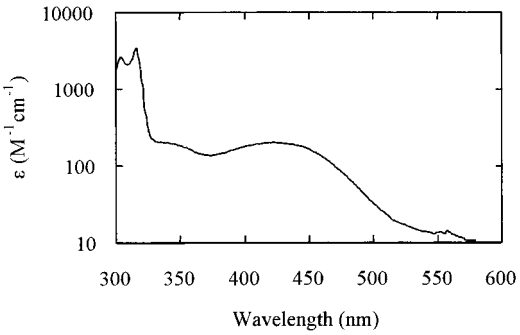

Figure 1. Absorption spectrum of the HMB/TCNB complex obtained by mixing stock solutions of acceptor and donor (ca. 2×10^{-2} M) at 25 °C in DCLE. The spectra of the unbound acceptor and donor were subtracted, assuming an association constant for complex formation of $K_{CT} = 9.07$ M^{-1}.

Solutions of TCNB and HMB (both 10^{-2} M) were placed in a quartz cuvette with 1,2-dichloroethane (DCLE) as the solvent. At these concentrations, the samples consisted mainly of 1:1 complexes and 2:1 complex formation has been shown to be negligible.[39] Ground-state absorption spectra were obtained using a Beckman DU 640 UV−vis spectrometer. For time-resolved measurements, the samples were stirred using a magnetic stirrer and 200 pulse pairs were averaged for each delay setting. The resultant time-resolved curves were fit using a custom simplex computer routine to find the nonlinear least-squares minimum of the error between a model function and the observed data trace.

The calculation of structures and electronic properties of the complex followed standard procedures using HyperChem[40] release 5.0 on a 420 MHz IBM-compatible personal computer equipped with a Pentium II processor.

Materials. TCNB was purchased from Aldrich Chemical Co. and was purified by passing it through silica gel twice with dichloromethane as the elution solvent followed by recrystallization twice from chloroform. HMB was purchased from Aldrich Chemical Co. and purified by passing it through alumina with DCLE as the elution solvent followed by recrystallization from ethanol. DCLE used in the spectroscopic experiments was purchased from Sigma as HPLC-grade and was used without further purification.

Results

The ground-state absorption spectrum of the HMB/TCNB complex, free from residual absorbance due to the unbound acceptor and donor, is shown in Figure 1. This spectrum was obtained by mixing stock solutions of acceptor and donor (ca. 2×10^{-2} M) at 25 °C in DCLE. The spectra of the individual unbound acceptor and donor were then subtracted, assuming an association constant for complex formation of $K_{CT} = 9.07$ M^{-1}.[41]

Picosecond pump−probe transient absorption spectra were obtained at very short time delays ($t \sim 0$ ps) and at relatively long delays ($t \sim 300$ ps). The shape of the absorption spectrum does not change significantly within this time scale.[42] An example of the transient spectrum obtained 100 ps after 355 nm excitation is shown in Figure 2. The band at 468 nm has been assigned previously to a TCNB radical anion produced within the laser pulse.[8−10,42]

The decay trace for the HMB/TCNB CT complex after excitation with 355 nm light was recorded and is shown in

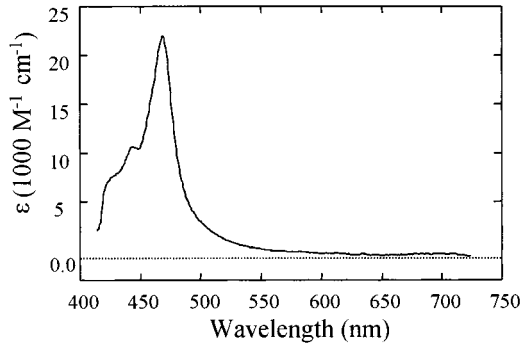

Figure 2. Picosecond pump−probe transient absorption spectrum obtained 100 ps after 355 nm excitation of the HMB/TCNB CT complex. The band with a maximum at 468 nm has been assigned previously to the TCNB radical anion produced within the laser pulse.

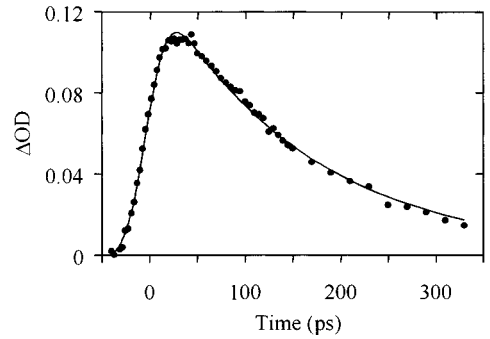

Figure 3. Picosecond pump−probe transient absorption decay trace obtained using 355 nm excitation of the HMB/TCNB CT complex and observed at 468 nm polarized at the magic angle (filled circles). The line indicates the best fit of the observed trace using a single-exponential decay.

Figure 3. The excitation used was linear-polarized along the laboratory *Z* axis, and the probe beam was linearly polarized at 54.7° with respect to the laboratory *Z* axis. Thus, this trace does not contain dichroic information but is due to the formation and decay of the ion pair convoluted with the instrument response function. The rapid relaxation process for this complex has been reported to be ca. 5 ps in acetonitrile.[43] This process is much too rapid to be resolved by these experiments and need not be included in the kinetic scheme. However, the effect of relaxation on the alignment of the products relative to the ground-state CT complex will be recorded in the observed dichroism. The currently accepted model of the dynamics of photochemically produced ion pairs requires the ion-pair decay to be fit to a two-exponential function with an offset. In an effort to reduce the number of adjustable parameters, the magic angle trace was analyzed as a single-exponential decay.[44] The results were as follows: $A_1 = 0.1377$ (OD units), $k_1 = 6.28 \times 10^9$ s^{-1} with an instrument response function of 35 ps, assuming a Gaussian profile. The fitted line is also included in Figure 3.

Two additional decay traces were recorded and are shown in Figure 4. In the first trace (open circles), the probe beam was linear-polarized along the laboratory *Z* axis (i.e., parallel to the excitation), and in the second (filled circles), the probe beam was polarized within the laboratory *xy* plane (i.e., perpendicular to the excitation). Except for the polarization of the probe beam, all three traces (Figures 3 and 4) were collected under identical conditions. The shape of the traces shown in Figure 4 is due to a composite of the ion-pair decay and the randomizing rotations of the ion pairs in solution superimposed on the instrument response profile of the laser system. The dichroic traces were fit, assuming a single-exponential anisotropy component in addition to the parameters obtained from the magic angle data. Thus, both dichroic traces were simultaneously fit using only three adjustable parameters, i.e., a rate constant and two preexponential factors. The rate constant obtained was $k_{OR} = 1.33 \times 10^{10}$ s^{-1}, and the preexponential factors were $A_{(\parallel)} = -0.0364$ (OD units) for the parallel trace and $A_{(\perp)} = 0.0181$ (OD units) for the perpendicular trace.

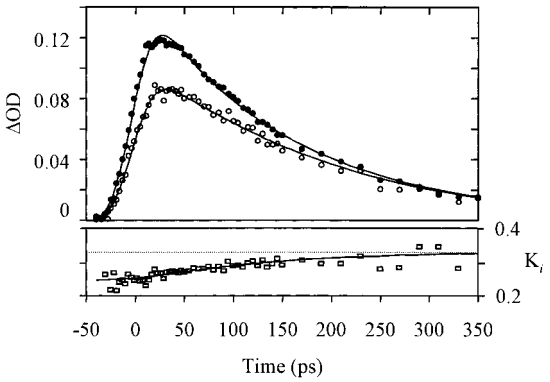

Figure 4. Top panel: Picosecond pump−probe transient absorption decay traces obtained using 355 nm excitation of the HMB/TCNB CT complex and observed with 468 nm light polarized parallel (open circles) and perpendicular (filled circles) to the excitation. The lines show the best fit of the individual dichroic traces, assuming a single-exponential decay component to the dichroism decay, in addition to the parameters obtained by fitting the magic angle trace (Figure 3). Bottom panel: Plot of the orientation factor as a function of time calculated using the above dichroic traces (open boxes). The solid line indicates the fit of the orientation factor on the basis of the parameters obtained from the fit of the individual traces above. The dashed line indicates a *K* value of 0.333.

Changing the excitation wavelength to 394 or 443 nm does not affect the observed traces, nor does changing the probe wavelength to 460 or 480 nm, because identical dichroism traces were recorded in all cases.

Discussion

TRLD. The fitting of the traces shown in Figure 4 resulted in the determination of one time constant and two preexponential factors that describe the magnitude and time course of the observed dichroic effect. The time constant is related to the average molecular rotational diffusion rate constant as defined by Debye−Stokes−Einstein diffusion theory.[46] Accordingly, as the molecules rotate, the orientation factors of the principal axes must converge at $K_X = K_Y = K_Z = 0.333$ and the sample becomes isotropic again. The K_i value is also required to converge at 0.333, and it does, as can be observed in Figure 4. The experimental value of the time constant obtained by fitting the data is $\tau_{OR} = 75 \pm 15$ ps. The theoretical value, assuming stick boundary conditions and assuming a spherical shape, can be predicted using eq 2[46]

$$\tau_{OR} = \eta_s V/RT \qquad (2)$$

Substituting η_s as the viscosity of the solvent in poise, *V* as the molar volume of the complex in milliliters per mole, *R* as the gas constant in ergs per mole Kelvin, and the absolute temperature (*T*) gives τ_{OR} in units of seconds. Numerical evaluation of τ_{OR} for the HMB/TCNB complex results in a value of about 90 ps in DCLE at room temperature. The agreement between the observed and calculated rotation time constants suggests that the eventual loss of orientation is due to random rotational motion of the complex. This finding is in contrast to the tetracyanoethylene/pyrene CT complex, where a directed

CHART 1

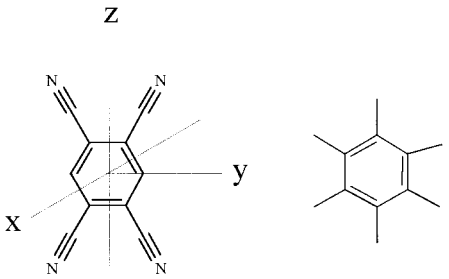

topochemical randomization due to the interconversion between different ion-pair structures has been observed.[20]

The preexponential factors allow the initial dichroism of the CRIP to be calculated. In this case, $d_i = 0.650 \pm 0.01$ for the HMB/TCNB complex and an orientation factor of $K_i = 0.245$ results. Using eq 1, the average angle between the ground-state CT transition moment and the TCNB radical anion transition moment, after relaxation, can be calculated: $\theta_{CRIP} = 70 \pm 4°$. This angle corresponds to the angle between the CT ground-state TMV and the TCNB radical anion absorption TMV *after* relaxation of the excited complex.

At this point, we have no information about how this angle relates to the molecular frame nor can we describe the effect the relaxation process has on the overall orientation of the sample. These topics will be addressed in the remaining discussion, which is organized as follows. We must first define the set of axis systems used to describe the relative orientations of the acceptor and donor. This is followed by a description of the structure of the ground-state complex and the prediction of the relevant TMV directions on theoretical considerations. Finally, the TRLD results are discussed in terms of the geometry of the CRIP relative to the starting CT complex and the relaxation of the excited state.

Defining the Axis Systems. Two different axis systems are used in the description of these results. The first axis system describes the orientation of the sample within the laboratory frame of reference. For this purpose, mutually orthogonal axes were depicted using uppercase letters *X*, *Y*, and *Z*. The photons used to excite the sample were linearly polarized with their electric vectors oriented parallel to the laboratory *Z* axis, and the direction of propagation was used to define the *X* axis. The probe pulse propagated in the *XY* plane, at a small angle with respect to the *X* axis, but its polarization direction was adjustable between the limits of being along the *Z* axis (parallel to the excitation) or in the *XY* plane (perpendicular to the excitation).

A second set of axes is needed to describe the molecular configurations of the donor and acceptor within the complex. Lowercase letters *x*, *y*, and *z* were used for this purpose. The origin was defined as the center of mass of TCNB, and the axes were defined as shown in Chart 1. The position of HMB within the ground-state complex was then determined relative to the TCNB center of mass.

Structure of the CT Complex. For insight into the structure of these weakly bound complexes, we turn to simple calculations and to crystallographic studies. Molecular mechanics (MM+), semiempirical (AM1), and ab initio (HF/321G*) methods were all used to predict the ground-state complex geometry. The calculated minimum energy structure of the CT complex according to ab initio calculations is shown in Figure 5. All three calculations qualitatively agreed with the structure as shown. The π planes of TCNB and HMB were predicted to be nearly parallel in all cases. The HMB center of mass was offset

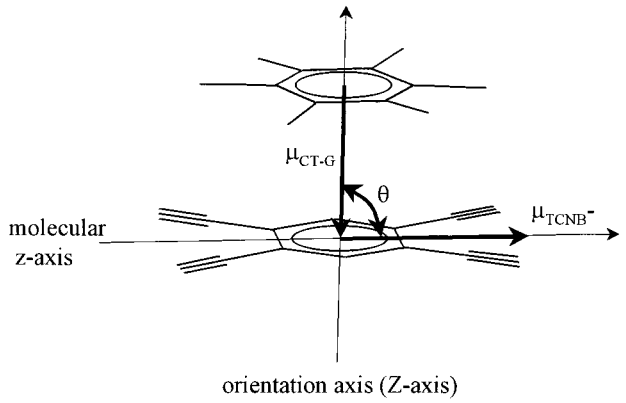

Figure 5. Calculated minimum energy geometry of the ground-state HMB/TCNB CT complex (ab initio HF/321G*) with the proposed ground-state TMV (μ_{CT-G}) and relaxed TMV (μ_{TCNB^-}) directions. The angle depicted is θ_{FC}.

along the *z* axis by between 0.33 and 0.38 Å in each case. Very little offset in the *y* direction was predicted by any of the calculations. The major difference among the calculations was the magnitude of the separation between the two ring systems with values of 3.52 (MM+), 4.94 (AM1), and 3.98 Å (ab initio).

The calculated structures also agreed qualitatively with the published crystal structure.[45] In accordance with the crystal structure, the TCNB/HMB planes were also nearly parallel and separated by 3.54 Å. A significant difference between the crystal and calculated structures concerns the magnitude of the observed offsets. In the crystal structure, the HMB was offset along the *z* axis by 0.91 Å, significantly larger than predicted by the calculations. An offset in the *y* direction and rotation of the HMB to a lower symmetry geometry were also observed in the crystal structure but not predicted by the calculations.

There is no a priori reason to believe that the crystal structure will be more accurate than the calculations in predicting the complex structure in solution. The influence of crystal-packing forces may not be negligible, particularly for these relatively weak complexes. Nevertheless, the fact that all of the structures are qualitatively similar does suggest that they collectively depict a reasonable geometry of this complex in a noninteracting solvent like DCLE. Consequently, we chose not to adopt a specific structure for the CT complex geometry. Instead we allow the offset in the *z* direction to vary between 0.35 and 0.90 Å, the offset in the *y* direction to vary between 0 and 0.7 Å, and the separation between the π planes to vary between 3.5 and 4.0 Å. Rotation of the HMB with respect to the TCNB *x* axis can be shown to be inconsequential.[46] Thus, the HMB center of mass is expected to fall within the rectangle defined by a diagonal between the points (4.0, 0, 0.35) and (3.5, 0.7, 0.9). All possible orientations of the HMB within this cube will be considered in the determination of the TMV directions.

CT Complex TMV. Mulliken theory gives insight into the possible TMV direction for the ground-state complex.[3,5−7] The two-state wave functions are usually depicted as follows:

$$\Psi_G = a(\Psi_{AD}) + b(\Psi_{A^-D^+}) \quad (3)$$

$$\Psi_{CTE} = a^*(\Psi_{A^-D^+}) - b^*(\Psi_{AD}) \quad (4)$$

where Ψ_G and Ψ_{CTE} are the wave functions for the ground state and CT excited state of the complex, respectively, and Ψ_{AD} and $\Psi_{A^-D^+}$ are the wave functions depicting the nonbonded interactions within the complex and the ion-pair state, respectively. Using these wave functions, the transition dipole for each

of the CT transitions may be evaluated using quantum theory and is given by[3,5−7]

$$\mu_{CT-G} = -e\int \Psi_{CT} \sum_i r_i \Psi_G \, d\tau \cong a^*b(\mu_1 - \mu_0) + (aa^* - bb^*)(\mu_{01} - \mu_0 S_{CT-G}) \quad (5)$$

where μ_1 and μ_0 are the dipole moments of the nonbonded and ion-pair states, respectively, and μ_{01} is the transition dipole between them. The term S_{CT-G} is shorthand notation for the overlap integral between the ground- and excited-state wave functions, and the coefficients *a*, *a**, *b*, and *b** are as defined above.

There are two experimental observations that justify the use of these simplified wave functions. Specifically, a detailed analysis of the absorption spectrum of the HMB/TCNB complex has shown that the localized excited states do not contribute significantly to the CT absorption.[39] The second observation is that excitation into several CT absorption bands leads to identical dichroic traces. The only reasonable explanation for this finding is that localized excitation (LE) intensity borrowing is negligible because it is unlikely that the LE would mix equally into several CT states. Thus, the interaction of localized states can be safely ignored, and the transitions in question are purely CT in nature.

Multiple acceptor and donor ion-pair states must be included in the model to account for the appearance of multiple CT absorption bands.[2,3,39,47,48] On the bright side, the energies of the molecular orbitals do not seem to change significantly because of complex formation. The observed maxima for the two absorption bands at ca. 345 and 425 nm correspond closely to the energy difference between the lowest unoccupied molecular orbital (LUMO) and the second-lowest unoccupied molecular orbital (SLUMO) of TCNB.[39] In addition, HMB has a degenerate set of highest occupied molecular orbitals (HOMOs). Perturbation due to complex formation should break this degeneracy, although perhaps not significantly. Hence, there are at least four MOs that must be considered, i.e., the second highest occupied molecular orbital (SHOMO), the HOMO, the LUMO, and the SLUMO of the complex. These orbitals are depicted in Figure 6, and they are readily identified as predominantly belonging to HMB (SHOMO and HOMO) and TCNB (LUMO and SLUMO) moieties. In each case, the calculated electron density on the adjoining (bare) ring system is small, although not zero, which is consistent with relatively weak transitions and low oscillator strengths.

It is convenient to use these molecular orbitals, depicted in Figure 6, as approximate wave functions in evaluating the transition-moment directions. The first term in eq 5 can be evaluated on the basis of the removal of an electron from the specified orbital of the donor and the placing of it into the specified orbital of the acceptor. Therefore, $\mu_1 - \mu_0 \sim e(\mathbf{r}_D - \mathbf{r}_{A^-})$, where $\mathbf{r}_D$ is the average position of the electron on HMB before transfer is initiated and $\mathbf{r}_{A^-}$ is the average position of the electron that resides on TCNB after the transfer is complete. The second term in eq 5 can be evaluated similarly such that $\mu_{01} - \mu_0 S_{CT-G} \sim eS_{CT-G}(\mathbf{r}_D - \mathbf{r}_{AD^-})$, where $\mathbf{r}_{AD^-}$ is the average position of the electron within the overlap region between TCNB and HMB. For centrosymmetric donors and acceptors such as HMB and TCNB, in the limit of small interaction energies, both terms in eq 5 amount to dipole moments directed between the centers of mass of the individual donor and acceptor molecules. This conclusion applies to the transition moments for all CT transitions for this complex regardless of the identity of the specific orbitals whose occupancy is changing. In other words, all of the CT TMV (μ_{CT-G}) will be directed from the center of mass of HMB to the center of mass of TCNB. As mentioned above, excitation at 355, 393, or 443 nm must excite several of the possible CT transitions to differing extents. At all three of these excitation wavelengths, identical dichroic traces were recorded. The only reasonable explanation for this observation is that all of the CT TMV are parallel.

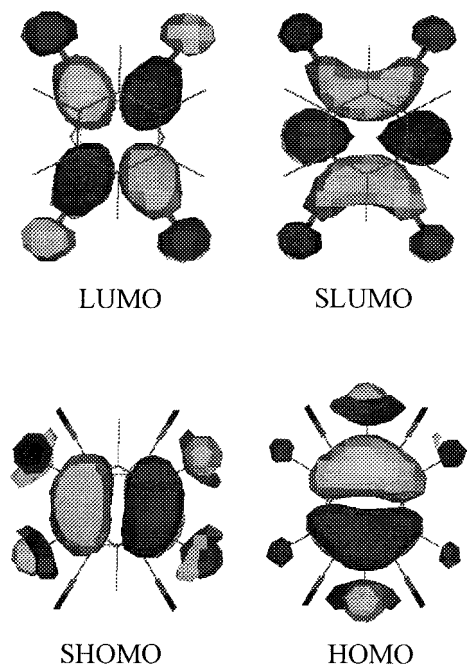

Figure 6. Calculated molecular orbital diagrams for the HMB/TCNB complex SHOMO, HOMO, LUMO, and SLUMO looking down the molecular *x* axis with HMB on top.

It is possible to pin the molecular frame onto the principal orientation axis now that the ground-state TMV direction is known. In this case, the unique uniaxial axis, the principal orientation *Z* axis, and the ground-state transition moment all correspond to the vector connecting the center of mass of HMB to the center of mass of TCNB. This is shown in Figure 5.

TCNB Radical Anion TMV. After excitation, the CT complex rapidly relaxes to a state characterized by an intense absorption due to the TCNB radical anion.[8−10,42] The transition at 468 nm is of $\pi-\pi^*$ character, and the transition moment is required by symmetry to be in the plane of the TCNB aromatic ring.[49] ZINDO/S calculations on the AM1-optimized geometry show that this transition dipole, μ_{TCNB^-}, is directed along the molecular *z* axis. This TMV direction is also included in Figure 5.

It is now a relatively simple matter to calculate the angle between the CT ground-state TMV and the TCNB radical anion absorption TMV *before* the relaxation of the FC state.[51] When the expected directions of μ_{CT-G} and μ_{TCNB^-} are taken into account, this angle falls between 76 and 84° for the entire range of possible geometries. Thus, $\theta_{FC} = 80 \pm 4°$. After relaxation, this angle is $\theta_{CRIP} = 70 \pm 4°$, on the basis of the measured value as determined above. Thus, there appears to a difference between the two angles because of relaxation.

Are these angles really different given the uncertainty in the ground-state geometry? If the angle in the ground-state geometry was actually 70°, the offset along the *z* axis required approaches 1.3 Å, assuming a 3.6 Å separation. This offset is significantly larger than that observed in the crystal structure and 4 times larger than that which the calculations predict. Considerably less than half of the aromatic ring systems could overlap effectively if the offset was this large. Even given the uncertainty

in the ground-state geometry, a 1.3 Å offset seems unreasonable. We are left to conclude that the relaxation process does cause a change in the observed angle.

Topochemical Analysis. Recall that an isotropic solution irradiated with light that is linearly polarized along the laboratory *Z* axis produces a uniaxially oriented sample of excited states by photoselection. Immediately following excitation, the *Z* axis in the laboratory frame, the unique orientation axis within the molecular frame, and the average direction of the TMV responsible for absorbing the photon, in this case μ_{CT-G}, all coincide. As the relaxation that converts the FC into the CRIP progresses, the average position of the molecular frame with respect to the orientation axis (and the laboratory *Z* axis) may change. The new position of the molecular frame can be related to the previous position by a sequence of successive rotations, as is defined by Euler angles. For uniaxially oriented samples, such as those of interest to the present discussion, all physical rotations that cause a significant change in the orientation of the sample, on average, can be defined in terms of a rotation through a single angle. We define this angle as the topochemical angle, and the rotation is described as causing a topochemical increment to the observed orientation.

If all molecules follow a single reaction path, knowledge of this path is sufficient to determine the topochemical angle. If multiple paths are possible, a weighted average of the resultant angles must be assumed. The information that can be obtained from these experiments is incomplete and will only partially define the topochemistry. They reveal nothing about the number of possible reaction paths and do not allow the complete set of Euler rotation angles to be determined. However, the magnitude of the topochemical angle can be sufficient evidence to disprove a possible mechanism on the basis of an analysis of the structures of the reactants and products and a description of the reaction path.[34] There are a few examples where an analysis of this type has been described in solution.[20,35−37]

The next step is to explore possible relaxation mechanisms and determine what effect the topochemical conversions would have on the initial geometry. One possibility would be to assume that a geometry change occurs on the excited surface. Such geometry changes have been postulated for similar CT complexes on the basis of photoacoustic measurements,[24] differences between the measured and calculated return electron-transfer rates,[27] and the unusually high reorganization energies associated with the excitation of CT complexes.[25,26,28] With a progression along these lines, it is best to assume the starting geometry is the offset geometry as described above and then require the CRIP to adopt a symmetrical structure, where the centers of mass are not offset in either the *z* or *y* directions. Next, we assume that the relaxation follows the direct reaction coordinate, with the two ring systems sliding past each other. Qualitative arguments can then be used to predict the final alignment of the product structure relative to the starting geometry, assuming isotropic solvent interactions. The entire complex must rotate in the laboratory frame such that the angle the TCNB *z* axis makes with the orientation axis (laboratory *Z* axis) would decrease upon going from the FC to the CRIP. This is exactly what was observed.

The relatively simple picture that emerges allows a self-consistent description of the excitation and relaxation processes of this complex to be established. It is clear that a minor change in the geometry because of relaxation can account for the discrepancies in the observed and predicted angles. It is important to note that other possible relaxation processes, for example, an electronic relaxation or even solvent reorganizations, that are accompanied by a geometric change cannot be ruled out. Furthermore, not all geometry changes will result in an observed topochemical increment. Specifically, only the vector components of the molecular motions perpendicular to the orientation axis (the ground-state TMV and the *Z* axis) will produce an observable topochemical change. Motion along the orientation axis or rotation around this axis cannot be assessed. Nevertheless, it does appear that a geometry change is associated with the relaxation process.

Conclusions

The application of TRLD spectroscopy to the study of the rapid relaxation process of the excited HMB/TCNB CT complexes has been presented. The observed dichroism is used to determine the angle between the ground-state CT transition moment and the product, TCNB radical anion, absorption moment after the relaxation is complete. This angle is compared with the expected angle on the basis of a calculated ground-state structure and the transition moments predicted by theory. The difference between the measured and predicted angles is consistent with a geometry change after excitation. It was further suggested that the ion pair adopts a symmetrical configuration after relaxation from an initial offset geometry. The TRLD results are compatible with these assumed geometries and with the relatively small geometry change required to interconvert them.

Acknowledgment. The authors are grateful for the support of this work by NSF (CHE-9985299) and the University of Maryland, Baltimore County, DRIF.

References and Notes

(1) Gould, I. R.; Young, R. H.; Farid, S. In *Photochemical Progress in Organized Molecular Systems*; Honda, K., Ed.; Elsevier: Amsterdam, The Netherlands, 1991.
(2) Foster, R. *Organic Charge-Transfer Complexes*; Academic Press: New York, 1969.
(3) Mulliken, R. S.; Person, W. B. *Molecular Complexes*; Wiley: New York, 1969.
(4) Chanon, M.; Hawley, M. D.; Fox, M. A. Introduction. In *Photoinduced Electron Transfer*; Fox, M. A., Chanon, M., Eds.; Elsevier: New York, 1988.
(5) (a) Mulliken, R. S. *J. Am. Chem. Soc*. **1950**, *72*, 600. (b) Mulliken, R. S. *J. Am. Chem. Soc*. **1950**, *72*, 4493. (c) Mulliken, R. S. *J. Chem. Phys.* **1951**, *19*, 514.
(6) Mulliken, R. S. *J. Am. Chem. Soc*. **1952**, *74*, 811.
(7) Mulliken, R. S. *J. Chem. Phys*. **1955**, *23*, 397.
(8) Miyasaka, H.; Ojima, S.; Mataga, N. *J. Phys. Chem.* **1989**, *93*, 3380−3382.
(9) Ojima, S.; Miyasaka, H.; Mataga, N. *J. Phys. Chem*. **1990**, *94*, 4147−4152.
(10) Ojima, S.; Miyasaka, H.; Mataga, N. *J. Phys. Chem*. **1990**, *94*, 5834−5839.
(11) Mataga, N.; Murata, Y. *J. Am. Chem. Soc*. **1969**, *91*, 3144−3152.
(12) Kobayashi, T.; Yoshihara, K.; Nagakura, S. *Bull. Chem. Soc. Jpn.* **1971**, *44*, 2603−2610.
(13) Gould, I. R.; Noukakis, D.; Gomez-Jahn, L.; Young, R. H.; Goodman, J. L.; Farid, S. *Chem. Phys.* **1993**, *179*, 439−456.
(14) Findley, B. R.; Smirnov, S. N.; Braun, C. L. *J. Phys. Chem. A* **1998**, *102*, 6385−6389.
(15) Hayashi, M.; Yang, T.-S.; Yu, J.; Mebel, A.; Lin, S. H. *J. Phys. Chem. A* **1997**, *101*, 4156−4162.
(16) Jarzeba, W.; Murata, S.; Tachiya, M. *Chem. Phys. Lett*. **1999**, *301*, 347−355.
(17) Prochorow, J.; Deperasinska, I. *J. Mol. Struct*. **1998**, *450*, 47−58.
(18) Deperasinska, I.; Prochorow, J.; Dresner, J. *J. Lumin.* **1998**, *79*, 65−77.
(19) Dresner, J.; Prochorow, J.; Ode, W. *J. Phys. Chem*. **1989**, *93*, 671−677.
(20) Wynne, K.; Reid, G. D.; Hochstrasser, R. M. *J. Chem. Phys*. **1996**, *105*, 2287−2297.
(21) Okajima, S.; Lim, B. T.; Lim, E. C. *Chem. Phys. Lett*. **1985**, *122*, 82−86.

(22) Lim, B. T.; Okajima, S.; Chandra, A. K.; Lim, E. C. *J. Chem. Phys.* **1982**, *77*, 3902−3909.
(23) Gould, I. R.; Farid, S. *J. Am. Chem. Soc*. **1993**, *115*, 4814−4822.
(24) Wegewijs, B.; Paddon-Row, M. N.; Braslavsky, S. E. *J. Phys. Chem. A* **1998**, *102*, 8812−8818.
(25) Britt, B. M.; McHale, J. L.; Friedrich, D. M. *J. Phys. Chem*. **1995**, *99*, 6347−6355.
(26) Markel, F.; Ferris, N. S.; Gould, I. R.; Myers, A. B. *J. Am. Chem. Soc*. **1992**, *114*, 6208−6219.
(27) Kulinowski, K.; Gould, I. R.; Myers, A. B. *J. Phys. Chem*. **1995**, *99*, 9017−9026.
(28) Kelly, A. M. *J. Phys. Chem. A* **1999**, *103*, 6891−6903.
(29) Thulstrup, E. W.; Michl, J. *Spectroscopy with Polarized Light. Solute Alignment by Photoselection in Liquid Crystals, Polymers and Membranes*; VCH Publishers: Deerfield Beach, FL, 1986.
(30) Thulstrup, E. W.; Michl, J. *Elementary Polarization Spectroscopy*; VCH Publishers: Deerfield Beach, FL, 1989.
(31) Ansari, A.; Szabo, A. *Biophys. J*. **1993**, *64*, 838−851.
(32) Szabo, A. *J. Chem. Phys*. **1984**, *81*, 150−167.
(33) Magde, D. *J. Chem. Phys*. **1978**, *68*, 3717−3733.
(34) Arnold, B. R.; Balaji, V.; Downing, J. W.; Radziszewski, J. G.; Fisher, J. J.; Michl, J. *J. Am. Chem. Soc*. **1991**, *113*, 2910−2919.
(35) Sension, R. J.; Repinec, S. T.; Hochstrasser, R. M. *J. Phys. Chem*. **1991**, *95*, 2946−2948.
(36) Repinec, S. T.; Sension, R. J.; Szarka, A. Z.; Hochstrasser, R. M. *J. Phys. Chem.* **1991**, *95*, 10380−10385.
(37) Sension, R. J.; Repinec, S. T.; Szarka, A. Z.; Hochstrasser, R. M. *J. Chem. Phys.* **1993**, *98*, 6291−6315.
(38) Poliakov, P. V.; Arnold, B. R. *Spectrosc. Lett.* **1999**, *32*, 747−762.
(39) Arnold, B. R.; Zaini, R. Y.; Euler, A. *Spectrosc. Lett*. **2000**, *33*, 595−614.
(40) HyperChem is supplied by Hypercube Inc., 1115 NW 4th Street, Gainesville, FL 32601.
(41) Arnold, B. R.; Euler, A.; Fields, K.; Zaini, R. Y. *J. Phys. Org. Chem.* In press.
(42) Arnold, B. R.; Noukakis, D.; Farid, S.; Goodman, J. L.; Gould, I. R. *J. Am. Chem. Soc.* **1995**, *117*, 4399−4400.
(43) The relaxation time for this complex was measured in acetonitrile, but the toluene/TCNB complex was studied in several solvents, including acetonitrile and DCLE (see ref 8). On the basis of the minor solvent dependence observed in the toluene complex, the HMB/TCNB complex relaxation time in DCLE can be estimated to be ca. 5 ps.
(44) The interconversions between CRIP, SSRIP, and free radical ions require five parameters if the currently accepted model is used (see ref 42). The fact that the decay trace shown in Figure 3 was fit adequately to a single-exponential decay suggests that ion-pair separation is slow relative to back electron transfer. Thus, the rate of ion-pair decay can be equated with the back-electron-transfer rate from the CRIP.
(45) Niimura, N.; Ohashi, Y.; Saito, Y. *Bull. Chem. Soc. Jpn.* **1968**, *41*, 1815−1820.
(46) The rotation of HMB simply changes the degree of overlap between the combinations of orbitals and therefore the identity of the specific orbitals responsible for the observed absorption. Because this does not change the TMV direction within the molecular frame, it is not important in the context of the current discussion. However, under the assumption that the calculated structure is correct, the band at 425 nm would be due to the transition between the SHOMO and LUMO and the band at 345 nm would be due to the transition between HOMO and SLUMO. The other two possible transitions would not contribute significantly to the observed absorption.
(47) Frey, J. E. *Appl. Spectrosc. Rev.* **1987**, *23*, 247−283.
(48) Frey, J. E.; Aiello, T.; Fu, S.-L.; Hutson, H. *J. Org. Chem*. **1996**, *61*, 295−300.
(49) Masuhara, H.; Mataga, N. *Z. Physik. Chem.* (*Muenchen*) **1972**, *80*, 113−128.
(50) Fleming, G. R. *Chemical Applications of Ultrafast Spectroscopy*; Oxford University Press: New York, 1986; Chapter 6.
(51) The angle of interest is that between the vector connecting the origin to the HMB center of mass and the *z* axis. This angle is given by $|\theta| = \tan^{-1}(z/(x^2 + y^2 + z^2)^{-1})$ where *x*, *y*, and *z* are the coordinates of the HMB center of mass.